

## $Z$ -diagrams of Composite Objects<sup>\*</sup>

T. JAROSZEWICZ

*Physics Department  
University of California, Los Angeles  
Los Angeles, CA 90024*

and

STANLEY J. BRODSKY

*Stanford Linear Accelerator Center  
Stanford University, Stanford, California 94309*

### ABSTRACT

We examine the effect of particle compositeness on the importance of “ $Z$ -diagrams”, i.e., virtual particle-antiparticle states appearing in scattering processes. The examples of positronium in QED, and of the nucleon in the QCD-based quark model, are discussed in detail. Generally, if the composite particle consists of  $N$  constituents, its  $Z$ -diagram amplitude involves creation and annihilation of  $N$  constituent-anticonstituent pairs. This process (which we assume to be governed by Coulomb-type interactions with the “fine structure constant”  $\alpha$ ) must take place in a small volume  $\sim 1/M^3$ , where  $M$  is the particle’s mass; an additional suppression is due to the fact that the created system is electrically (or color-) neutral. The composite particles’  $Z$ -diagram amplitude is then suppressed, compared to that for an elementary particle, by at least a factor  $f_Z \sim (q^2/M^2)[\alpha^2/M^3 R^3]^{N-1}$ , where  $q$  is the momentum transfer to the particle, and  $R$  the composite particle’s size. The decoupling of the composite  $Z$ -diagrams at zero momentum transfer is consistent with low-energy theorems.

Submitted to *Physical Review C*

---

<sup>\*</sup> Work supported by the Department of Energy, contract DE-AC03-76SF00515.

## I. Introduction

The meson-nucleon relativistic quantum field theory, known as various versions of Quantum Hadrodynamics (QHD)<sup>1</sup> has become a much used tool in nuclear physics. It has found applications in the nuclear matter problem, the structure of finite nuclei, elastic and inelastic interactions of electrons and nucleons with nuclei, etc. (see, e.g., the reviews<sup>2</sup>).

One of the basic features of QHD is that, at least to the first approximation, nucleons are treated as elementary objects. In the full field-theory context, they are described in terms of a local, spin-1/2, Dirac field interacting with meson fields, so that, strictly speaking, nucleon structure arises only as a result of radiative corrections in higher orders in the perturbation theory (i.e., nucleons become “dressed” in a meson cloud). In the mean-field-theory limit nucleon wave functions satisfy then the Dirac equation for an elementary fermion, with external meson fields. Similarly, in scattering processes, the “Relativistic Impulse Approximation” (RIA)<sup>3</sup> assumes local interactions of the projectile nucleon with target nucleons, as if they were elementary.

The fact that nucleons have an internal structure cannot be, on the other hand, reasonably doubted. In principle, QHD can account at least partially for the nucleon structure in terms of radiative corrections, i.e., dressing the nucleon in a meson cloud. In practice, however, systematic computation of these effects in a strong-coupling field theory is prohibitively difficult; the commonly used approach is to simply multiply meson-nucleon vertices by phenomenological form-factors. On the one hand, this procedure, although somewhat ad hoc, seems reasonable, as the meson-nucleon field theory is, after all, only an effective, low-energy, theory with an inherent cut-off. On the other hand, the use of form-factors is most questionable in processes constituting the crucial difference between the non-relativistic and relativistic theories: these are the processes represented by “Z-diagrams”, in which virtual  $N\bar{N}$  pairs are created and annihilated (Fig. 1 (a)). Precisely the apparent presence of  $N\bar{N}$  pairs is responsible<sup>4</sup> for the improved description of scattering processes in the Relativistic Impulse Approximation. The difficulty with the straightforward use of

form-factors in the Z-diagrams is the following: The conventional nucleon form-factor, to be applied to meson-nucleon vertices, is a function  $F(q^2)$  of the meson four-momentum squared,  $q^2$ , and refers to on-mass-shell nucleons. This, however, is *not* the situation encountered in the Z-diagrams (Fig. 1 (a)): Those diagrams are time-ordered diagrams, in which the lines do not have definite four-momenta; when re-expressed in terms of covariant Feynman diagrams, they involve integrals over the time components of the four-momenta carried by the internal lines (for more details see Appendix A). The diagram of Fig. 1 (a), for instance, can be written as a term in the meson-nucleon scattering amplitude, integrated over the time component of the four-momentum  $p$ . Such an integral, involving both on- and off-mass-shell momenta of the intermediate state nucleon, cannot possibly be expressed in terms of nucleon form-factors alone. Only the nucleon-pole contribution to the integral can readily be evaluated. It is proportional to the product of the two form-factors at the meson-nucleon vertices, taken with *large* arguments  $\gtrsim 4M^2$ , i.e., is very strongly suppressed. There is, however, no reason to neglect other contributions to the integral, and these, especially for a composite system, dominate.

The above-mentioned relation between time-ordered and covariant diagrams will be discussed later in more detail; at present we may conclude that the Z-diagrams depend in an intricate way on the dynamical mechanisms of meson-nucleon interactions, and their evaluation requires much more information than just nucleon form-factors. In this paper we analyze the Z-diagrams, i.e., the processes of creation and annihilation of virtual nucleon-antinucleon pairs, in the framework of a definite dynamical model of a composite nucleon – the constituent quark model. Our ultimate aim is to establish to what extent are the meson-nucleon relativistic models compatible with the nucleon (and meson) compositeness, and what are the limits of their applicability.

One domain in which the “elementary-” and “composite-” nucleon pictures do automatically agree, is, expectedly, the region of momentum transfers small compared to the characteristic nucleon excitation energy. Physically, it may be expected that probing

the nucleon in this kinematical regime cannot possibly reveal its internal structure. This fact can be, more rigorously, expressed in terms of “low-energy theorems”, as discussed in detail in Ref. 5 for the low-energy (Thomson) limit<sup>6</sup> of forward Compton scattering on a composite system (see Appendix B for a summary of these results). In the context of nuclear physics, the low-energy theorems are applicable to nuclear processes at energy scales of tens of MeV.

The smallness of the momenta involved in the scattering process is, however, not a necessary condition for the composite nucleon to behave as if it were elementary. Situations in which, theoretically, scattering amplitudes involving nucleons should be insensitive to the nucleon’s internal structure may also occur in nucleon scattering on a nucleus for the laboratory nucleon momenta in the 1 GeV range; in that case, although the three-momentum transfer in the laboratory system is small, the energy of the exchanged mesons *in the nucleon rest system* may be substantial (see a more detailed discussion of kinematics in the following Section).

Such processes can be analyzed in analogy to the so-called “ $J = 0$  fixed-pole” amplitude for real Compton scattering on composite objects.<sup>7</sup> The results for Compton scattering have been generalized<sup>8</sup> to the case of *isoscalar* mesons interacting with the nucleon, described in the framework of the additive constituent quark model (in which mesons are assumed to couple locally to approximately point-like constituent quarks). In this model the *quark Z*-diagrams<sup>9</sup> (Fig. 1 (b)) reproduce approximately the point-like nucleon *Z*-diagram (Fig. 1 (a)). This result follows from the interplay of kinematics and combinatorics of diagrams, and can be physically understood as follows: First, the energy denominator in Fig. 1 (b) is approximately twice the quark (instead of nucleon) mass, as in Fig. 1 (a); since the effective constituent quark mass is about 1/3 the nucleon mass, the individual quark *Z*-diagrams are enhanced by the factor  $\simeq 3$ . Secondly, there are three distinct quark *Z*-diagrams; hence an additional enhancement by the factor of 3. Third, however, because of additivity of quark interactions, the meson-quark couplings are, for *isoscalar* mesons,

equal to  $1/3$  of corresponding meson-nucleon couplings; two meson-quark vertices yield, therefore, a suppression by the factor of 9. Finally, then, all these factors compensate:  $(3 \times 3)/9 = 1$ .

The quark model may thus explain why, for isoscalar interactions (which is the case for nucleon scattering on heavy isospin- or spin-zero nuclei), the Dirac equation (and RIA) may be applicable in spite of nucleon compositeness. These arguments break down, however, for isovector meson exchanges, since the group factors relating meson-quark couplings to meson-nucleon couplings are then entirely different, and also when the nucleon's momentum is not distributed equally between the three quarks. In any case, the physical picture is *completely different* than that suggested by the Dirac equation for nucleons: the relativistic effects manifest themselves through quark Z-diagrams rather than nucleon Z-diagrams.

The last statement can be formulated more strongly: it is not true that the Dirac equation with elementary nucleons, and the composite quark model, provide two "equivalent" or "complementary" descriptions of the same reality. On the contrary, even though *some* predictions of these two pictures may be identical or similar, the different physical mechanisms involved do give different results for other measurable quantities. Such a quantity is, for example, the number of antiquarks in the nucleus, as measured in deep-inelastic lepton scattering, or in the Drell-Yan process. In the elementary-nucleon model one calculates the Z-diagram amplitude (Fig. 1 (a)) as if the nucleons were point-like; this amplitude is a contribution to the probability of finding a  $N\bar{N}$  pair created by meson-exchange interactions with other nucleons in the nucleus. Now, since one has to accept that an antinucleon contains at least three (valence) antiquarks, the number of additional antiquarks in the nucleus will be at least three times the number of virtual antinucleons. In the composite-nucleon model, on the other hand, the Z-diagram amplitude is reproduced (for isoscalar interactions) by *quark* Z-diagrams (Fig. 1 (b)), so that the number of

antiquarks “per Z-diagram” is one instead of three, and the  $q\bar{q}$  sea enhancement is much smaller.

In this paper we concentrate on the above-mentioned observable consequences of the nucleon compositeness. In the framework of the QCD-based quark model, we consider a composite nucleon interacting with an elementary boson field, and estimate the probability of finding simultaneously the triplet of virtual quarks and antiquarks which corresponds to the Z-diagram for an elementary nucleon; it is, essentially, the configuration shown in Fig 1 (c). We define then the “nucleon Z-diagram suppression factor”  $f_Z$  as the ratio of this probability to that for point-like nucleons.

An alternative concept of the Z-diagram suppression has been introduced previously in Ref. 9. We reformulate this concept somewhat more precisely in Appendix A, and show there that it is qualitatively consistent with the suppression factor defined above.

Another order-of-magnitude estimate of the suppression factor, along the lines of our present approach, has been also given in Ref.8. As we discuss later (Appendix A), that estimate gives only a weak upper bound on the suppression factor; the reason is that it includes a large class of diagrams that cannot be interpreted as contributions to the composite particle Z-diagram. Physically, the stronger suppression we find now is due to additional color-weight cancellations.

The paper is organized as follows: In Sec. II we formulate the ideas mentioned above in more detail: we describe kinematics of nuclear interactions, discuss time-development of nuclear processes in terms of appropriate Fock-space states, and arrive at an expression for the Z-diagram suppression factor in terms of time-ordered diagrams involving  $q\bar{q}$  creation due to gluon exchanges.

In the following we evaluate  $f_Z$ ; but, as an introduction to the calculation in the quark model, we first consider (Sec. III) Z-diagrams for a simple and well-understood system: the positronium in an external (say, Coulomb) field. In that case we are able to easily calculate the suppression factor  $f_Z$ , and to express it in terms of the fine structure constant: to the

lowest order,  $f_Z \sim \alpha^5 q^2/M^2$ , where  $M$  is the positronium mass, and  $q$  the momentum transferred to it in the process of virtual pair creation. That calculation is then extended, in Sec. IV, to a QCD-type quark model, in which  $q\bar{q}$  pairs are created by gluon exchanges. We conclude, in Sec. V, with a general discussion of the role of virtual  $N\bar{N}$  pairs in nuclear processes.

## II. Statement of the problem

Although Z-diagrams for composite objects are typically analyzed in the context of Compton scattering, we shall rather discuss circumstances typical of nuclear interactions. Generally, we consider a composite object of mass  $M$ , interacting with an external, static, scalar or vector potential. To be concrete, we may think of it a nucleon in a meson field generated by nucleons in a heavy nucleus; that picture is adequate for a nuclear matter problem in the mean-field approximation, as well as for nucleon scattering on a heavy nucleus in the optical-potential limit. For a vector potential we can then assume that only its time component is non-zero. To avoid further complications we will treat the meson field as elementary.

The interaction of the nucleon with the meson field can be now described in terms of amplitudes for (virtual) meson scattering on the nucleon, so that kinematics of these processes has to be considered. Generally, since the meson field is static in the nuclear rest system, the four-momentum of the meson is  $q = (0, \vec{q})$ , with  $\vec{q}$  small compared to the nucleon mass  $M$ . Its square,  $q^2 = -\vec{q}^2$ , is thus also small compared to  $M^2$ . Another relevant invariant involved in the meson-nucleon amplitudes is  $s \equiv (K + q)^2$ , the total four-momentum squared of the meson-nucleon system. It is more convenient to use, instead of this quantity, the meson energy  $\omega$  in the *nucleon* rest system; its relation to  $s$  is

$$s = M^2 + q^2 + 2M\omega$$

for an on-mass-shell nucleon. At the same time, if the nucleon three-momentum in the nuclear rest system is  $\vec{K}$ , then we also have

$$s = M^2 + q^2 - 2\vec{K} \cdot \vec{q} ,$$

hence,

$$\omega = -2 \frac{\vec{K} \cdot \vec{q}}{M} . \tag{2.1}$$

It follows then from Eq.(2.1) that in the nuclear matter problem, when  $|\vec{K}|$  is of the order of the Fermi momentum, the equivalent meson energy  $\omega$  is small compared to the nucleon excitation energy, and low-energy theorems apply. On the other hand, in intermediate-energy nucleon-nucleus scattering (at projectile nucleon laboratory momenta in the GeV range),  $\omega$  may be substantial, and the fixed-pole analysis is applicable.

To summarize, looking at the meson-nucleon scattering amplitudes in the nucleon rest system, we are concerned with slightly space-like meson four-momenta, and with meson energies smaller than or comparable to the typical nucleon excitation energy (few hundred MeV).

Having specified the kinematics, we must now decide what precisely should be meant by a nucleon Z-diagram for a composite nucleon. The definition has to be phrased in terms of the time-development of the meson-nucleon system, i.e., in terms of intermediate states occurring in the time-ordered diagrams representing the meson-nucleon scattering amplitude.<sup>10</sup> To be physically acceptable, such a definition should correspond as closely as possible to the time evolution of the meson-nucleon system for a *point-like* nucleon. The essential feature of the latter process is that, in the time interval between the creation and annihilation of the  $N\bar{N}$  pair, the nucleons and antinucleons do not interact with each other (Fig. 1 (a)). Thus, if we want to reproduce this physical picture in the quark model, we should only take into account diagrams in which every additional  $q\bar{q}$  pair is created by a gluon originating from the already existing  $q\bar{q}$  pair, the first  $q\bar{q}$  pair originating from the meson; an analogous requirement applies to  $q\bar{q}$  pair annihilation. An example of such a

process is shown in Fig. 2 (a), where  $q\bar{q}$  pairs are created in a “cascade” from the first pair, and all the gluon exchanges take place *within* the  $qqq$  and  $\bar{q}\bar{q}\bar{q}$  systems representing the nucleons and antinucleons. In contrast, in the diagram of Fig. 2 (b) one of the  $q\bar{q}$  pairs is created by a gluon originating from the nucleon. Because of color, this gluon exchange causes the intermediate state (indicated by the vertical broken line in the diagram) to be very different than the  $N\bar{N}$  system appearing in the original Z-diagram (Fig. 1 (a)) we are trying to simulate. Although the intermediate state in question is an overall color singlet, its internal color structure is, in general, completely different than that of the three separate color singlets representing the  $N\bar{N}$  state. Another way of looking at the diagram of Fig. 2 (b) is to interpret the  $q\bar{q}$  pair created by the incoming nucleon as a contribution to the nucleon’s  $q\bar{q}$  sea, unrelated to the virtual  $N\bar{N}$  pair creation process, and independent of the fact that the nucleon is interacting with the meson field. In any case, the quark diagram of Fig. 2 (b), “translated” into a diagram involving hadronic states, does not reproduce the original hadronic Z-diagram of Fig. 1 (a).

The last point to be addressed in this Section is our definition of the Z-diagram suppression factor  $f_Z$  in the meson-nucleon interaction. We simply define  $f_Z$  as the absolute value of the ratio of two amplitudes: that of the diagrams shown in Fig. 2 (a), and that of the diagram of Fig. 1 (a) calculated for a point-like nucleon. In the following we assume, for simplicity, isoscalar mesons (for isovector mesons the results remain, qualitatively, the same). Now, since for isoscalar mesons (as discussed in the Introduction) the point-like nucleon diagram of Fig. 1 (a) is approximately equal to that of Fig. 1 (b), we can equally well calculate  $f_Z$  as the ratio of the diagrams of Fig. 2 (a) to those of Fig. 1 (b), i.e., symbolically,

$$f_Z = \left| \frac{\text{Fig. 2 (a)}}{\text{Fig. 1 (b)}} \right|.$$

### III. Positronium Z-diagram

Before estimating the suppression factor  $f_Z$  in the quark model, let us consider a simpler case of QED, and calculate approximately the suppression factor for the Z-diagram of the positronium. Elements of the calculation for this example will be used in the following Section.

The counterpart of the diagram of Fig. 1 (b) for the positronium is the Z-diagram of a single electron,<sup>11</sup> shown in Fig. 3. The relevant parts of the positronium Z-diagrams, analogous to those of Fig. 2 (a), are those shown in Fig. 4. In all these diagrams the additional  $e^+e^-$  pair is created by a photon emitted from the already existing pair, and  $e^+e^-$  pair annihilation processes have an analogous property.

In an approximate calculation of the diagrams of Fig. 4 some simplifications can be now made. In analogy to the nuclear-physics problem, we assume that the external three-momenta  $\vec{q}$  are small compared to the electron mass  $m$ . Consequently, since the positronium is a loosely bound system, and all the diagrams considered are ultra-violet convergent, we can safely make non-relativistic approximations in the kinematics. A simple analysis shows then that the upper bound on the suppression factor  $f_Z$  can be obtained by simply ignoring all spin factors, and calculating the diagrams of Fig. 4 as for scalar particles. This approximation can be justified as follows:

A time-ordered Z-diagram for a spin-1/2 particle, with momenta as in Fig. 1 (a), is proportional to a matrix element of the negative-energy part of the Dirac propagator, taken between spinors of the incoming and outgoing particle,

$$\bar{u} \gamma_0 G^{(-)}(\vec{p}) \gamma_0 u = \bar{u} \gamma_0 \frac{E(\vec{p}) \gamma_0 + \vec{p} \cdot \vec{\gamma} - m}{2 E(\vec{p}) [E + E(\vec{p})]} \gamma_0 u , \quad (3.1)$$

where  $E$  is the energy of the incoming and outgoing particle,  $E(\vec{p}) \equiv \sqrt{m^2 + \vec{p}^2}$ , and the factors  $\gamma_0$  appear, because the external potential is assumed to be the time-component

of a four-vector. Now, for  $|\vec{p}| \lesssim m$  we can set  $E \simeq E(\vec{p}) \simeq m$ , and interpret the resulting approximate expression (3.1) as

$$\frac{1}{2m} \left[ \bar{u} \gamma_0 \frac{E(\vec{p}) \gamma_0 + \vec{p} \cdot \vec{\gamma} - m}{2m} \gamma_0 u \right],$$

where the factor  $(2m)^{-1}$  is the inverse of the approximate energy denominator associated with the intermediate state, and the expression in the square brackets is a dimensionless “spin factor”, which would be equal 1 for the analogous diagram with spinless particles (we normalize spinors to  $\bar{u} u = 1$ ). Now, if all momenta  $\vec{k}$  are small compared to  $m$ , the spin factor is proportional to  $|\vec{k}|/m < 1$ .

Similar estimates can be given for Z-diagrams ordered not in time, but in the light-plane variable  $x_+ \equiv t + z$ . In this case we have to use that part of the Dirac propagator which describes propagation backwards in the variable  $x_+$ ,

$$G^{[-]}(\vec{p}) \simeq \frac{1 - \gamma^3}{2m},$$

for  $|\vec{p}| \ll p_0 \simeq m$ . Consequently, for three-momenta small compared to  $m$ , the spin factor is now approximately equal 1. Thus, when we neglect spin, we can only overestimate Z-diagrams, both  $t$ - and  $(t + z)$ -ordered.

We can proceed now to evaluating the diagrams of Fig. 4, including all possible, topologically distinct, orderings of vertices. Each of these diagrams, compared to the diagram of Fig. 3, involves two extra energy denominators, equal approximately  $2m$ . Besides, the original energy denominator ( $\simeq 2m$ ) of the diagram of Fig. 3 is replaced now by  $\simeq 4m$ . In addition to these factors, the diagrams of Fig. 4 involve photon-exchange interactions, which, for a nonrelativistic bound system, such as the positronium, can be described by the Coulomb potential. Integrating over positions of the vertices can be then also simplified: We may note that, because of short life-times ( $\sim 1/m$ ) of the intermediate states, the coordinates of the electron and the positron remain practically unchanged during the pair creation/annihilation process, i.e.,  $\vec{r}_1 \simeq \vec{r}'_1$ , and  $\vec{r}_2 \simeq \vec{r}'_2$  (Fig. 4 (a1)). Thus, the

expression corresponding to the sum of diagrams of Fig. 4 has simply to be averaged with the positronium wave functions squared,  $|\psi(\vec{r})|^2$ , where  $\vec{r} \equiv \vec{r}_{12} \equiv \vec{r}_1 - \vec{r}_2$ .

Now, by looking at the diagrams of Fig. 4, we realize that there are systematic partial cancellations between them. The physical reason is that, say, the pair at the position  $\simeq \vec{r}_2$  is created by a photon emitted from the first pair – which is a system of zero charge, and similarly for annihilation. Therefore, the diagram (a1) is partially cancelled by (a2) and (a3), (a2) is partially cancelled by (a1) and (a4), etc. Physically, the additional pair is created (annihilated) by photons emitted (absorbed) by an electric dipole of a varying orientation, and, consequently, the photon-exchange interaction has a limited range. The resulting effective short-range potential can be approximately evaluated as follows (see Fig. 5):

Let us consider, in momentum space, a Coulomb photon of momentum  $\vec{p}$  emitted from an  $e^+e^-$  pair of vanishing initial total momentum (in our diagrams we assume small  $\vec{q}$ ). The relevant part of the diagram involves thus an energy denominator corresponding to the  $e^+e^-$  intermediate state, and the photon-exchange potential  $\tilde{V}(\vec{p})$ . The Fourier transform of this expression can be then interpreted as the effective “dipole” potential  $U(\vec{r})$  divided by the approximate energy denominator  $2m$ . For a given momentum  $\vec{k}$  of the positron in the  $e^+e^-$  pair we have thus

$$\int \frac{d^3p}{(2\pi)^3} \left[ \left( 2m + 2 \frac{\vec{k}^2}{2m} \right)^{-1} - \left( 2m + 2 \frac{(\vec{k} + \vec{p})^2}{2m} \right)^{-1} \right] \tilde{V}(\vec{p}) = \frac{1}{2m} U_{\vec{k}}(\vec{r}), \quad (3.2)$$

with  $\tilde{V}(\vec{p}) = 4\pi\alpha/\vec{p}^2$ . The potential  $U$  defined in this way depends, of course, on the momentum  $\vec{k}$ ; in particular, for  $\vec{k} = \vec{0}$  we have

$$U_{\vec{0}}(\vec{r}) = \int \frac{d^3p}{(2\pi)^3} \frac{\vec{p}^2}{2m^2 + \vec{p}^2} \tilde{V}(\vec{p}) = \frac{\alpha}{r} e^{-\mu r}, \quad (3.3)$$

with  $\mu^2 = 2m^2$ . Alternatively, since the three-momenta are assumed to be small compared to the mass  $m$ , we can expand the integrand in Eq.(3.2) up to terms  $\sim \vec{p}^2/m^2$  and  $\vec{k}\cdot\vec{p}/m^2$ , and obtain

$$U_{\vec{k}}(\vec{r}) \simeq \int \frac{d^3p}{(2\pi)^3} \frac{2\vec{k}\cdot\vec{p} + \vec{p}^2}{2m^2} \tilde{V}(\vec{p}) = \frac{2\pi\alpha}{m^2} \left[ \delta^3(\vec{r}) + \frac{i}{2\pi} \frac{\vec{k}\cdot\vec{r}}{r^2} \right].$$

Generally,  $U_{\vec{k}}(\vec{r})$  has the range  $\sim 1/m$ , its integral over a small volume about the origin is

$$\int d^3r U_{\vec{k}}(\vec{r}) \simeq \frac{2\pi\alpha}{m^2},$$

and its  $\vec{k}$ -dependence is, to the lowest order in  $1/m$ , negligible. In the following we take thus, for simplicity,

$$U(\vec{r}) = \frac{\alpha}{r} e^{-\mu r}. \quad (3.4)$$

In terms of the effective short-range potential  $U(\vec{r})$  we can then represent all the diagrams of Fig. 4 as a sum of just two terms (Fig. 6). There is also a partial cancellation between these two diagrams, simply because in one of them the outgoing external photon is attached to the  $e^-$ , and in the other to the  $e^+$  line. Their sum is thus proportional to the factor  $1 - \exp(i\vec{q}\cdot\vec{r}_{12}) \equiv 1 - \exp(i\vec{q}\cdot\vec{r})$ .

Collecting all the factors discussed above, we find, then,

$$f_Z \lesssim \frac{2m}{4m} \frac{1}{(2m)^2} \int d^3r |\psi(\vec{r})|^2 U^2(\vec{r}) \left(1 - e^{i\vec{q}\cdot\vec{r}}\right). \quad (3.5)$$

After expanding the exponent in powers of  $\vec{q}$ , and substituting the positronium wave function  $|\psi(r)|^2 = (\alpha^3 m^3 / 8\pi) \exp(-\alpha m r)$ , we find, for  $q^2 \equiv \vec{q}^2 \ll m^2$ ,

$$f_Z \lesssim \frac{q^2}{(4m)^2} \int d^3r |\psi(\vec{r})|^2 \alpha^2 e^{-2\mu r} \simeq \frac{q^2}{(4m)^2} |\psi(\vec{0})|^2 \frac{\pi\alpha^2}{\mu^3},$$

or

$$f_Z \lesssim \frac{\alpha^5 q^2}{256 \sqrt{2} m^2}. \quad (3.6)$$

We can also write, in terms of the positronium Bohr radius  $R = 2(\alpha m)^{-1}$ , and positronium mass  $M \simeq 2m$ ,

$$f_Z \lesssim \frac{q^2}{\sqrt{2} M^2} \frac{\alpha^2}{M^3 R^3}. \quad (3.7)$$

Let us stress again that the smallness of  $f_Z$  is only in part due directly to the weakness of the electromagnetic interaction. In Eq.(3.6) the exchange of two photons yields only the factor  $\alpha^2$ . The remaining three powers of  $\alpha$  are due to two reasons: first, the original  $e^+e^-$  pair, created by the external photon, and the secondary  $e^+e^-$  pair both have spatial extent  $\sim 1/m$ ; secondly, the secondary pair is created by a photon emitted by the first pair, which is a neutral object. Consequently, all the creation and annihilation processes must take place in a small volume  $\sim 1/M^3$ , much smaller than the overall positronium volume ( $\sim R^3$ ). Thus, the Z-diagram for the positronium can be represented as in Fig. 7, which emphasizes the spatial relationships between the extent of the positronium wave function, and the pair creation volume. The factor  $(MR)^{-3} \sim \alpha^3$  in Eq.(3.7) represents then (up to a numerical coefficient) the probability of finding the electron and the positron in the positronium at a relative distance  $\sim 1/M$ .

Finally, let us clarify the origin of the factor  $q^2/M^2$  in  $f_Z$ . As seen from Fig. 6, it is due to a partial cancellation of diagrams with different ordering of pair annihilation (or creation) vertices, the cancellation being almost complete when the external photon has zero momentum ( $q = 0$ ). In that case two relevant parts of the diagrams are shown in Fig. 8 for given three-momenta of the electrons and positrons. These two contributions enter with opposite signs, because the internal photon couples either to the electron or a positron line, so that the sum is proportional to the difference of the inverses of the corresponding energy denominators,

$$\frac{1}{2\varepsilon(\vec{k}_2)} - \frac{1}{2\varepsilon(\vec{k}_1)}, \quad (3.8)$$

with  $\varepsilon(\vec{k}) = \sqrt{m^2 + \vec{k}^2}$ . Since the three-momenta are small,  $\vec{k}^2 \sim R^{-2}$ , the difference (3.8) is also small, of the order  $m^{-1}(mR)^{-2}$ . In other words, for  $q = 0$ , the suppression factor

is of the order  $(MR)^{-2}$  relative to the leading contribution (i.e., that for  $q \neq 0$ ). Since our estimates give only the leading term in  $(MR)^{-1}$ , consistency requires that this nonleading term should be neglected. As we shall discuss later, the vanishing of the composite Z-diagram at  $q = 0$  is in agreement with low-energy theorems.

#### IV. Nucleon Z-diagram in a QCD-based quark model

Of most interest for nuclear physics is, clearly, to determine the Z-diagram suppression factor for a nucleon. We give below an estimate of  $f_Z$ , based on a simple model of a nucleon as a nonrelativistic bound state of constituent quarks, having (within the confinement radius) effective masses  $m \simeq M/3$ . We assume that the interaction responsible for creation of  $q\bar{q}$  pairs is a Coulomb-type one-gluon-exchange potential, whose spatial dependence is  $V(r) = \alpha_s/r$ . The last assumption does not imply that we believe the confining forces to be of the same type. In fact, our results should be independent of the confinement mechanism, and other nonperturbative phenomena. The reason is that the process of creation of a triplet of  $q\bar{q}$  pairs can only take place when all the quarks involved are located in a small volume, of size less than  $1/M$ , and therefore smaller than the confinement radius. It is then plausible that, well within the confinement region,  $q\bar{q}$  creation can be treated perturbatively. An essential assumption made here is that the interaction potential  $V(r)$  has the color structure corresponding to the standard coupling of a gluon to quarks in  $SU(3)_C$ .

Although it is a simplification that we concentrate on the effects of *nucleon* compositeness, and consider mesons as point-like objects, coupled locally to constituent quarks, it is justified, to some extent, by the phenomenologically successful “additive quark model” based on just this assumption. Also, our treatment of quarks (including created  $q\bar{q}$  pairs) as massive, “dressed”, constituent quarks, and not almost massless current quarks, is in line with the treatment of baryon-meson couplings in the  ${}^3P_0$  and similar quark models.

Some elements of the analysis have been discussed in the case of the QED example. The case of the QCD is, however, significantly more difficult, primarily because of a much larger set of diagrams that have to be included, because of the color group structure, and because of the obvious fact that the diagrams considered are six-loop diagrams. We do not attempt, therefore, a precise evaluation of  $f_Z$ , and rather stress the physical mechanisms, similar to those operating on the QED case, that tend to inhibit virtual  $q\bar{q}$  creation within the nucleon. By extrapolating the result for the positronium (two constituents) to the case of three constituents, we expect that

$$f_Z \sim \frac{q^2}{M^2} \left( \frac{\alpha_s^2}{M^3 R^3} \right)^2,$$

and that expectation is confirmed. Although our estimate is only approximate, we take care to include relevant numerical factors, and make sure that the numerical coefficient in the above proportionality is not anomalously large.

It would take too much space to list explicitly all the diagrams contributing to  $f_Z$ . We can, however, organize them in a way exhibiting partial cancellations, and introduce an effective short-range potential as in the QED case. With this in mind, let us look at some diagrams, shown in Fig. 9. The first one, (a), for example, is partially cancelled by the second, (b), etc. More precisely, the color group weights of all the diagrams in question are identical in absolute values. For example, the diagram (a) has the group structure shown in Fig. 10, where the quark-gluon vertices represent Gell-Mann matrices  $\frac{1}{2} \lambda_{ij}^a$ , and to the point where three quark lines meet, there corresponds the antisymmetric symbol  $\epsilon_{ijk}$ , coupling three quarks to a color singlet;  $i, j, k$  here are quark color indices, and  $a$  is an octet gluon index. By utilizing the usual group identities for the  $\lambda$ -matrices we find, as indicated in Fig. 10, that the color weight of the diagram (a) is  $(2/3)^4$  of the group weight of the corresponding diagram with no gluons, in particular for the single-quark Z-diagram. Therefore, the factor  $(2/3)^4$  will appear as one of coefficients in the Z-diagram suppression factor  $f_Z$ .

For each diagram shown in Fig. 9 we have indicated in parantheses the sign of its group weight relative to the group weight of the diagram (a). It is these signs that determine the cancellation pattern. For example, since the diagrams (a) and (b) enter with opposite signs, the gluon emitted from the color-singlet system at  $\vec{r}_1$ , and creating a  $q\bar{q}$  pair at  $\vec{r}_2$ , can be represented as the “color dipole” potential  $U_{12} \equiv U(\vec{r}_{12})$  of Eq.(3.4). It is less obvious that, since the diagrams (a) and (c) also have opposite color weights, the gluon exchange between the quark systems at  $\vec{r}_2$  and  $\vec{r}_3$  can be, similarly, represented as  $U_{23}$ . Further, adding the diagrams (d) and (e) yields the short-range potential  $U_{13}$  acting between the subsystems at  $\vec{r}_1$  and  $\vec{r}_3$ . [Actually, the effective potential responsible for creation of “second generation”  $q\bar{q}$  pairs (at  $\vec{r}_3$ ), has a shorter range than the potential  $U$  for the “first generation” pairs; if we use the same range, we only overestimate  $f_Z$ .] Next, since the diagrams (a) and (d) have the *same* sign, then, if we add (a), (b), ..., (e), and other 11 diagrams needed to complete the sum, the result will be proportional to  $+U_{12}(U_{23} + U_{13})$ . Similarly, since the diagrams (a) and (f) have the same sign of the group weights, while (f) and (g) have opposite signs, their sum, after adding another set of necessary diagrams, will yield  $+U_{13}(U_{12} - U_{23})$ . The last set of diagrams shown in Fig. 9, complemented with other necessary diagrams, gives  $-U_{23}(U_{13} + U_{12})$ , where the signs result from the relative signs of (a) and (h), and (h) and (i).

The diagrams considered above can be then symbolically represented as in Fig. 11 (a1), (a2), and (a3). These comprise one-half of all possible and distinct vertex orderings and gluon line arrangements. The other half, shown in Fig. 11 (b1), (b2), and (b3), have opposite group weights, and partly (or exactly, if  $\vec{q} = 0$ ) cancels the previous set, in analogy to the cancellation exhibited in Fig. 7. Summing all these diagrams, including the group weight, the factor  $2m/6m$  (because the original energy denominator  $2m$  in the single-quark Z-diagram is replaced by  $6m$ ), and the factor  $1/(2m\ 4m)^2$  (resulting from

additional energy denominators), we obtain, finally,

$$f_{\mathbf{z}} \lesssim \frac{2m}{6m} \frac{1}{(2m)^2} \frac{1}{(4m)^2} \left(\frac{2}{3}\right)^4 \left\langle U_{12}(U_{13} + U_{23}) \left[ U_{12}(U_{13} + U_{23}) (1 - e^{i\vec{q}\cdot\vec{r}_{12}}) \right. \right. \\ \left. \left. + U_{13}(U_{12} - U_{23}) (1 - e^{i\vec{q}\cdot\vec{r}_{13}}) \right. \right. \\ \left. \left. - U_{23}(U_{12} + U_{13}) (e^{i\vec{q}\cdot\vec{r}_{12}} - e^{i\vec{q}\cdot\vec{r}_{13}}) \right] \right\rangle. \quad (4.1)$$

Because of our special choice of the ordering of vertices, this expression is not manifestly symmetric in the three quark coordinates, but it has to be averaged with a symmetric wave function. After taking permutations of some variables we obtain, then,

$$f_{\mathbf{z}} \lesssim \frac{1}{3} \frac{1}{(8m^2)^2} \left(\frac{2}{3}\right)^4 \left\langle Q_{12} [U_{12}^2 (U_{13}^2 + U_{23}^2) + U_{13}^2 U_{23}^2] \right\rangle, \quad (4.2)$$

where  $Q_{ij} \equiv 1 - \cos(q r_{ij})$ .

Eq.(4.2) exhibits now the dependence on relative coordinates  $\vec{r}_{ij} \equiv \vec{r}_i - \vec{r}_j$  in a factorized form. Calculation of the averages is relatively simple, if we also assume a factorized Hulthén-type wave function;

$$\psi(r_{12}, r_{23}, r_{31}) = \psi_0 e^{-\beta(r_{12} + r_{23} + r_{31})/2}, \quad (4.3)$$

normalized such that

$$\int d^3 r_1 d^3 r_2 d^3 r_3 \delta^3(\vec{r}_1 + \vec{r}_2 + \vec{r}_3) |\psi(r_{12}, r_{23}, r_{31})|^2 = 1.$$

We can use then the formula

$$\int d^3 r_1 d^3 r_2 d^3 r_3 \delta^3(\vec{r}_1 + \vec{r}_2 + \vec{r}_3) f_{12}(\vec{r}_{12}) f_{23}(\vec{r}_{23}) f_{31}(\vec{r}_{31}) \\ = \frac{1}{3} (2\pi)^{-3} \int d^3 k \tilde{f}_{12}(\vec{k}) \tilde{f}_{23}(\vec{k}) \tilde{f}_{31}(\vec{k}), \quad (4.4)$$

where the Fourier transforms are defined as

$$\tilde{f}(\vec{k}) \equiv [f(\vec{r})]_{\vec{k}} = \int d^3 r e^{i\vec{k}\cdot\vec{r}} f(\vec{r}). \quad (4.5)$$

With the approximation  $1 - \cos(qr) \simeq q^2 r^2/2$  in Eq.(4.2), the Fourier transforms we need are

$$\begin{aligned} [e^{-\beta r}]_k &= \frac{8\pi\beta}{(\beta^2 + k^2)^2}, \\ [r^2 e^{-\beta r}]_k &= \frac{96\pi\beta(\beta^2 - k^2)}{(\beta^2 + k^2)^4}, \\ [r^2 U^2(r) e^{-\beta r}]_k &= \alpha_s^2 \frac{8\pi\beta_2}{(\beta^2 + k^2)^2}, \\ [U^2(r) e^{-\beta r}]_k &= \alpha_s^2 \frac{4\pi}{k} \arctan \frac{k}{\beta_2}, \end{aligned}$$

with  $\beta_n = \beta + n\mu$ . Eq.(4.2) can be then written as

$$\begin{aligned} f_Z \lesssim \frac{1}{3} \frac{1}{(8m^2)^2} \left(\frac{2}{3}\right)^4 \frac{128}{3} \pi \alpha_s^4 \psi_0^2 q^2 \int_0^\infty dk \left[ \frac{\beta\beta_2 k}{(\beta^2 + k^2)^2 (\beta_2^2 + k^2)^2} \arctan \frac{k}{\beta_2} \right. \\ \left. + \frac{3\beta(\beta^2 - k^2)}{(\beta^2 + k^2)^4} \left(\arctan \frac{k}{\beta_2}\right)^2 \right]. \quad (4.6) \end{aligned}$$

In the limit  $\beta \ll \mu$  the integral appearing here can be calculated in an elementary way, and the two terms give contributions  $\sim 1/\mu^4$ ,

$$\int_0^\infty dk [\dots] = \frac{\pi}{2(2\mu)^4} \left[ 1 + O\left(\frac{\beta^2}{\mu^2}\right) \right] \quad (4.7)$$

[in fact, for the nucleon,  $\beta$  is smaller than  $\mu$ , but not much smaller; therefore our estimate is only approximate].

Further, the coefficient  $\psi_0$  in the wave function (4.3) can be related to mean-square radius of the nucleon,  $R^2$ , defined by

$$\langle e^{i\vec{q}\cdot\vec{r}_3} \rangle = 1 - \frac{1}{6} R^2 q^2 + O(q^4). \quad (4.8)$$

With the wave function (4.3) we find the relations

$$R^2 = \frac{12}{7\beta^2},$$

and

$$\psi_0^2 = \frac{6}{7\pi^2} \left( \frac{12}{7R^2} \right)^3. \quad (4.9)$$

After substituting Eqs. (4.7) and (4.9) into Eq.(4.6), we find, in terms of the nucleon mass  $M$ ,

$$f_Z \lesssim \frac{2^5 3^6}{7^4} \frac{q^2}{M^2} \left( \frac{\alpha_s^2}{M^3 R^3} \right)^2 \simeq 9.7 \frac{q^2}{M^2} \left( \frac{\alpha_s^2}{M^3 R^3} \right)^2. \quad (4.10)$$

Since, experimentally, the isoscalar charge radius of the proton is  $R \simeq 0.72 \text{ fm} \simeq 3.6 \text{ GeV}^{-1}$ , the dimensionless expansion parameter appearing in  $f_Z$  is  $MR \simeq 3.4$ . Thus, numerically,

$$f_Z \lesssim 0.006 \alpha_s^4 \frac{q^2}{M^2}, \quad (4.11)$$

i.e., for any reasonable values of the momentum transfer and the strong coupling constant, composite nucleon Z-diagrams are suppressed, compared to either elementary nucleon- or single quark Z-diagrams, by at least a factor of 100. Physically, this suppression is mainly due to color cancellations, inhibiting creation of  $q\bar{q}$  pairs by a color singlet object. Because of these cancellations,  $q\bar{q}$  pair creation processes required in the nucleon Z-diagram can only take place when all quarks are located at relative distances smaller than the nucleon size. That physical picture is thus entirely analogous to that for the positronium Z-diagrams (see discussion at the end of Sec. III, and Fig. 7).

## V. Conclusion

Let us summarize the results of this paper by emphasizing again that although the Dirac equation may be, in some special circumstances, used to describe scattering of nucleons (or other composite objects), its applicability is quite limited:

First, the approximate numerical equivalence between the quark and point-like nucleon Z-diagrams is not universal<sup>8</sup>; it depends on the properties of interactions.

Secondly, even when quark Z-diagrams *do* reproduce point-like nucleon Z-diagrams in small momentum-transfer nuclear scattering, the physical mechanism of interaction is completely different than implied by the Dirac equation. That difference is not only the matter of interpretation, so that the elementary-nucleon and quark pictures are *not* equivalent (“dual”) descriptions of the same reality. In contrast, they lead to different observable consequences in other processes. For example, in a picture of composite nucleons relativistic effects in nuclear matter are due almost entirely to virtual  $q\bar{q}$  pairs, not  $N\bar{N}$  pairs. Therefore, the number of antiquarks in the nucleus (which can be measured, e.g., in the Drell-Yan process) increases, due to relativistic effects, much less than if nucleons were treated as point-like. It is exactly the square of our nucleon Z-diagram suppression factor  $f_Z$  which gives the relative probability of finding in the nucleus virtual  $N\bar{N}$ -like  $3(q\bar{q})$  states, compared to  $q\bar{q}$  states.

As we have mentioned before, the smallness of the suppression factor  $f_Z$  is essentially of geometrical origin. It is due mostly to the fact that the virtual  $q\bar{q}$  pairs have to be created and annihilated in the small volume ( $\sim 1/M^3$ ) occupied by the fluctuation. Besides, the created system of virtual quarks and antiquarks is an overall color singlet, and it has to originate from color-singlet hadrons, which leads to a significant suppression due to the color weights. It is also reassuring to note that the estimates obtained here in the framework of the quark model are qualitatively consistent with a different concept of Z-diagram suppression, considered in Ref. 9 (see Appendix A).

### Acknowledgments

This research was supported in part by the Department of Energy under contracts number DE-AC03-76SF00515 (S.J.B.) and number FG03-88ER40424 (T.J.).

## Appendix A. Z-diagrams in terms of Feynman diagrams

Following the method of Ref. 12, we establish here a relation between the time-ordered Z-diagram, and certain contributions to the covariant meson-nucleon scattering amplitude.

Let us first write the meson-nucleon amplitude (Fig. 12 (a)) as a sum of the nucleon pole term, and other contributions,

$$A(K, q) = g^2 F^2(q^2) \frac{1}{(K + q)^2 - M^2 + i0} + (\text{non-pole terms}) , \quad (\text{A.1})$$

where  $g$  is the meson-nucleon coupling constant, and  $F$  the nucleon form-factor (for simplicity we neglect here spin). If mesons are absorbed and emitted at space-time points  $x$  and  $y$ , the Z-diagram corresponding to Fig. 12 (a) is defined by requiring  $x_0 \geq y_0$ , i.e., by multiplying the covariant diagram (in configuration space) by the step function

$$\Theta(x_0 - y_0) = \int \frac{dl_0}{2\pi} e^{-i l_0 (x_0 - y_0)} \frac{i}{l_0 + i0} = \int \frac{d^4 l}{(2\pi)^4} (2\pi)^3 \delta^3(\vec{l}) e^{-i l (x - y)} \frac{i}{l_0 + i0} .$$

According to the last expression, in momentum space the vertices have to be connected by a line (Fig. 12 (b)) representing an “theton” – a fictitious particle carrying only energy  $l_0$ , and having the propagator  $i/(l_0 + i0)$ . The Z-diagram corresponding to the amplitude (A.1) is thus given by

$$A_Z(K, q) = \int \frac{d^4 l}{(2\pi)^4} (2\pi)^3 \delta^3(\vec{l}) \frac{i}{l_0 + i0} A_Z(K, q + l) ,$$

or, for  $q_0 = 0$ ,

$$A_Z(K, q) = \int \frac{dl_0}{2\pi} \frac{i}{l_0 + i0} \frac{g^2 F^2(l_0^2 - \vec{q}^2)}{(K_0 + l_0 - \varepsilon + i0)(K_0 + l_0 + \varepsilon - i0)} + (\text{non-pole terms}) , \quad (\text{A.2})$$

where, for  $\vec{q}^2 \ll M^2$ , the on-mass-shell energy of the intermediate-state antinucleon is

$$\varepsilon \equiv \sqrt{M^2 + (\vec{K} + \vec{q})^2} \simeq K_0 \equiv E .$$

The (anti)nucleon-pole contribution is then obtained by closing the integration contour around the pole at  $l_0 = -K_0 - \varepsilon + i0$ ,

$$A_Z(K, q) = -\frac{g^2}{2\varepsilon(K_0 + \varepsilon)} F^2((K_0 + \varepsilon)^2 - \vec{q}^2) \simeq -\frac{g^2}{4E^2} F^2(4E^2) + (\text{non-pole terms}) . \quad (\text{A.3})$$

The pole part of the Z-diagram is thus suppressed by the factor

$$f_Z^{\text{Pole}} \sim F^2(4E^2) < F^2(4M^2) , \quad (\text{A.4})$$

in agreement with Ref. 9.

To compare this suppression factor with that defined and evaluated in the text, we assume now that the composite system in question is bound by long-range (Coulomb-type) interactions, so that, for weak binding,  $MR \sim 1/\alpha$ . The suppression factor estimated in the text becomes then

$$f_Z \sim \frac{q^2}{M^2} \left( \frac{\alpha^2}{M^3 R^3} \right)^{N-1} \sim \frac{q^2}{M^2} (M^5 R^5)^{-(N-1)} ,$$

whereas, with the power counting rules<sup>13</sup> giving  $F(q^2) \sim (R^4 q^4)^{-(N-1)}$ , the pole contribution of Eq.(A.4) is

$$f_Z^{\text{Pole}} \sim (M^4 R^4)^{-(N-1)} .$$

In spite of this difference, both concepts of composite system's Z-diagrams give then consistently strong suppression, and, qualitatively, result in the same physical picture. The concept discussed in the text is preferable, since it takes into account color cancellations, and it pertains to physical Fock-space states, more directly related to measurable quantities (the distribution of antiquarks in the nucleon).

Both suppression factors,  $f_Z$  and  $f_Z^{\text{Pole}}$ , are, on the other hand, smaller than the estimate given in Ref. 8. The latter was obtained simply as the *inclusive* probability of finding in the system  $(N - 1)$  extra constituent-anticonstituent pairs in addition to the

pair associated with the constituent interacting with the external field. That probability was shown to be

$$f_Z^{\text{incl}} \sim \left( \frac{\Delta M}{M} \right)^{2(N-1)},$$

where  $\Delta M \sim \alpha^2 M \sim (MR^2)^{-1}$  is the typical excitation energy of the system. The suppression factor obtained in this way,

$$f_Z^{\text{incl}} \sim (M^4 R^4)^{-(N-1)},$$

is, apparently, of the same order as  $f_Z^{\text{Pole}}$ , but, as shown by a more careful analysis, it involves a very large numerical coefficient, due to a large number of diagrams that have to be taken into account. In contrast, in the more restricted class of diagrams considered in the present work, there are systematic cancellations due to group weights.

## Appendix B. The low-energy theorem and composite systems

We have shown in this paper that Z-diagrams involving the propagation of composite systems are suppressed in the degree depending on the degree of compositeness of the system. At first sight, this seems to be in conflict with the low-energy theorem for forward Compton scattering<sup>6</sup> which states that, for any charged target p, the  $\omega \rightarrow 0$  limit of the amplitudes is

$$A_{\gamma\text{P} \rightarrow \gamma\text{P}}(\omega) = -\frac{e^2}{M} \epsilon \cdot \epsilon' + O(\omega),$$

where  $\epsilon$  and  $\epsilon'$  are photon polarization vectors. The apparent discrepancy stems from the fact that, in QED, the entire contribution to the  $\gamma e \rightarrow \gamma e$  amplitude is given (in radiation gauge) by the electron Z-diagram. It is thus illuminating to understand the dynamics which restore the exact low energy limit in the case where the target is not an elementary object.

Detailed analyses of this problem have been given in the literature.<sup>5,7</sup> The essential time-ordered diagrams are shown in Fig. 13. We assume that the target is a bound state

of spin one-half elementary particles with charges  $e_i$ ,  $i = 1, 2, \dots, N$ . The contribution of the constituent Z-diagrams (Fig. 13 (a)) is then proportional to  $\sum_{i=1, \dots, N} e_i^2 / E_i$ , where  $E_i$  is an effective bound state energy of the constituent  $i$ .

The diagrams of Fig. 13 (b) and (c) involve a double sum over the currents of the constituents. After transforming those products to commutator terms, one can see that, at threshold, only the diagram (b) results in a non-vanishing “zero over zero” expression, the zero denominator being due to the intermediate ground state. By using sum rules, one can show that this contribution gives precisely the difference between the constituent Z-diagram contribution and the correct total amplitude, which is only dependent on the total charge  $e$  and total mass of the target. The above analysis can be extended to the relativistic domain using a Fock state expansion at equal “time”  $x_+ = t + z$  on the light-plane.

Thus the *constituent* Z-diagrams play an essential role in the scattering amplitude even at zero momentum transfer and very low energies. In contrast, the Z-diagram of the *composite* target as a whole (and its antiparticle) is negligible in the low energy limit. In fact, the vanishing of  $f_Z$  at zero momentum transfer is necessary, since the low-energy amplitude is obtained entirely from the constituent Z-diagram and the pole diagram 13 (b).

In the case where the photon has only isoscalar interactions  $e_i = e/N$  and assuming we can approximate  $E_i = M/N$ , the entire contribution to the low energy amplitude comes from the constituent Z-diagrams; this is another example of how the constituent Z-diagrams can mimic the Z-diagram contribution of the target, as discussed in Ref. 8. At threshold the physics is indistinguishable whether the target is elementary or not; however when the energy  $\omega$  is of the order of the target excitation energy and/or the momentum transfer is of the order of the inverse size of the target, the constituent nature of the target obviously gives a completely different description of the scattering amplitude compared to the naive Dirac treatment. In the case of interactions of a nucleon interacting in a background

meson field, such energies and momentum transfers are involved for contributions beyond the first Born approximation. The use of the Dirac equation to describe the dynamics of a composite nucleon in these circumstances is thus clearly invalid.

## References and Footnotes

- <sup>1</sup> J.D. Walecka, *Ann. Phys. (N.Y.)* **83**, 491 (1974).
- <sup>2</sup> M.R. Anastasio, L.S. Celenza, W.S. Pong, and C.M. Shakin, *Phys. Reports* **100**, 327 (1983); J.W. Negele, *Comments Nucl. Part. Phys.* **14**, 303 (1985); B.D. Serot and J.D. Walecka, *Advances in Nucl. Phys.* **16**, 1 (1986); L.S. Celenza and C.M. Shakin, *Relativistic Nuclear Physics: Theories of Structure and Scattering*, World Scientific Lecture Notes In Physics, vol. 2 (1986); G.E. Brown, W. Weise, G. Baym and J. Speth, *Comments Nucl. Part. Phys.* **17**, 39 (1987).
- <sup>3</sup> R.J. Shepard, J.A. McNeil, and S.J. Wallace, *Phys. Rev. Lett.* **50**, 1443 (1983); B.C. Clark, S. Hama, L.R. Mercer, L. Ray, and B.D. Serot, *Phys. Rev. Lett.* **50**, 1644 (1983).
- <sup>4</sup> M.V. Hynes, A. Picklesimer, P.C. Tandy, and R.M. Thaler, *Phys. Rev. Lett.* **52**, 978 (1984); *Phys. Rev.* **C31**, 1438 (1985).
- <sup>5</sup> S.J. Brodsky and J.R. Primack, *Ann. Phys. (N.Y.)* **52**, 315 (1969).
- <sup>6</sup> F.E. Low, *Phys. Rev.* **96**, 1428 (1954); M. Gell-Mann and M.L. Goldberger, *Phys. Rev.* **96**, 1433 (1954).
- <sup>7</sup> M. Gell-Mann, M.L. Goldberger, and W. Thirring, *Phys. Rev.* **95**, 1612 (1954); M.L. Goldberger and F.E. Low, *Phys. Rev.* **176**, 1778 (1968); S.J. Brodsky, F.E. Close, and J.F. Gunion, *Phys. Rev.* **D5**, 1384 (1971), *Phys. Rev.* **D8**, 3678 (1973).
- <sup>8</sup> E. Bleszynski, M. Bleszynski, and T. Jaroszewicz, *Phys. Rev. Lett.* **59**, 423 (1987).
- <sup>9</sup> S.J. Brodsky, *Comments Nucl. Part. Phys.* **12**, 213 (1984).
- <sup>10</sup> The quantities measured in deep-inelastic scattering and the Drell-Yan process are, in fact, related to the Fock-space states defined not at fixed time, but rather at a fixed light-plane variable. As discussed in the next Section, our estimates apply to time-ordered as well as "light-plane-ordered" diagrams.

- <sup>11</sup> To be more precise, to all diagrams we consider explicitly we have to add diagrams in which the electron and positron are interchanged. Thus, because of charge conjugation invariance, all amplitudes have to be multiplied by 2. That coefficient, however, cancels in the suppression factor defined as a ratio of amplitudes.
- <sup>12</sup> T. Jaroszewicz, J. Kwieciński, L. Leśniak, and K. Zalewski, *Phys. Lett.* **79B**, 127 (1978).
- <sup>13</sup> S.J. Brodsky and B.T. Chertok, *Phys. Rev. Lett.* **37**, 269 (1976); *Phys. Rev.* **D14**, 3003 (1976).

## Figure Captions

Fig. 1 Z-diagram of a point-like nucleon interacting with an external potential (a), the corresponding Z-diagram of a single quark (b), and the composite Z-diagram of the three-quark system (c).

Fig. 2 Gluon-exchange mechanisms of  $q\bar{q}$  pair creation. The diagram (a), and similar diagrams, reproduce the structure of the diagram of Fig. 1 (a), while the diagram (b) does not.

Fig. 3 The Z-diagram of a single electron in the positronium.

Fig. 4 Composite Z-diagrams for the positronium.

Fig. 5 Partially cancelling diagrams generating the effective short-range interaction potential.

Fig. 6 The diagrams of Fig. 4 represented in terms of the effective short-range interaction.

Fig. 7 Another representation of the process of Fig. 6 (a), suggesting a small pair-creation volume compared to the large positronium size.

Fig. 8 Elements of the diagrams of Fig. 6, responsible for cancellation at  $q = 0$ .

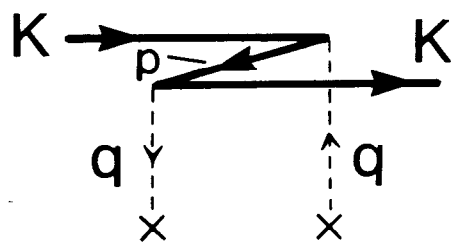
Fig. 9 Some quark-gluon diagrams contributing to the composite nucleon Z-diagram, together with the signs of their color group weights, relative to the diagram (a).

Fig. 10 The color group structure of the diagrams of Fig. 9.

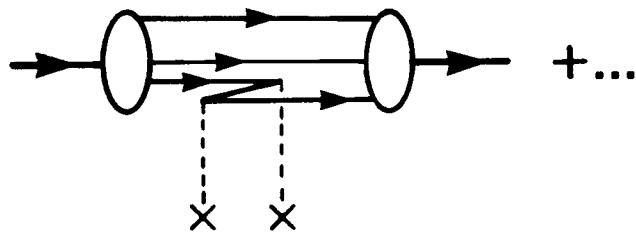
Fig. 11 The diagrams of Fig. 9 in terms of the effective short-range interaction.

Fig. 12 The meson-nucleon scattering amplitude (a), and the related covariant representation of the time-ordered Z-diagram (b).

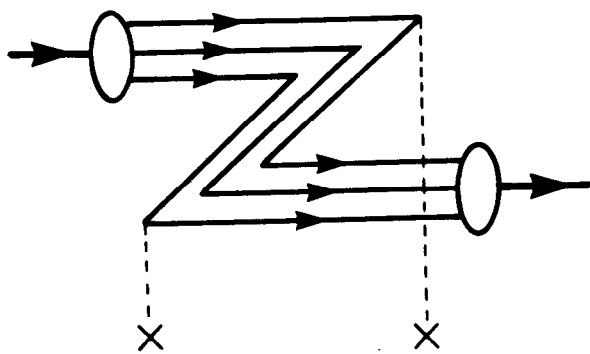
Fig. 13 Diagrams contributing to the forward Compton scattering in the low energy limit.



(a)

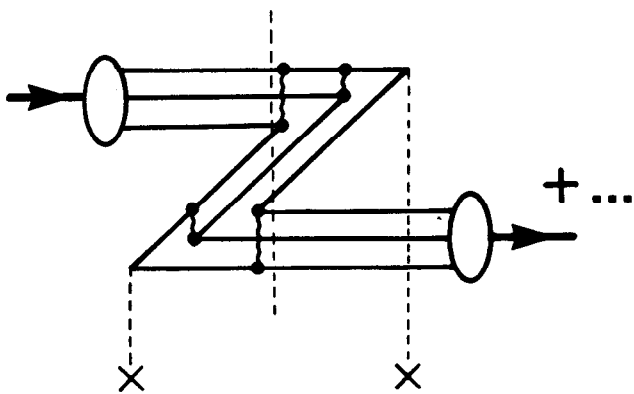


(b)

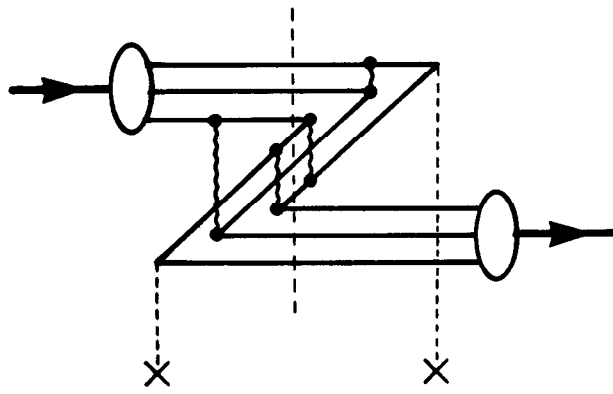


(c)

Fig. 1



(a)



(b)

Fig. 2

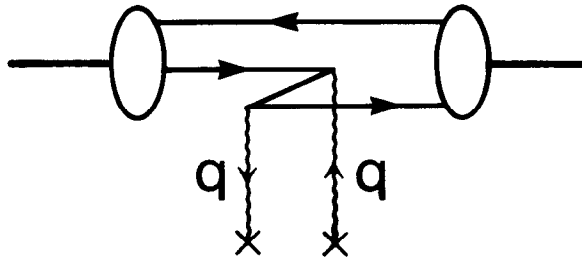


Fig. 3

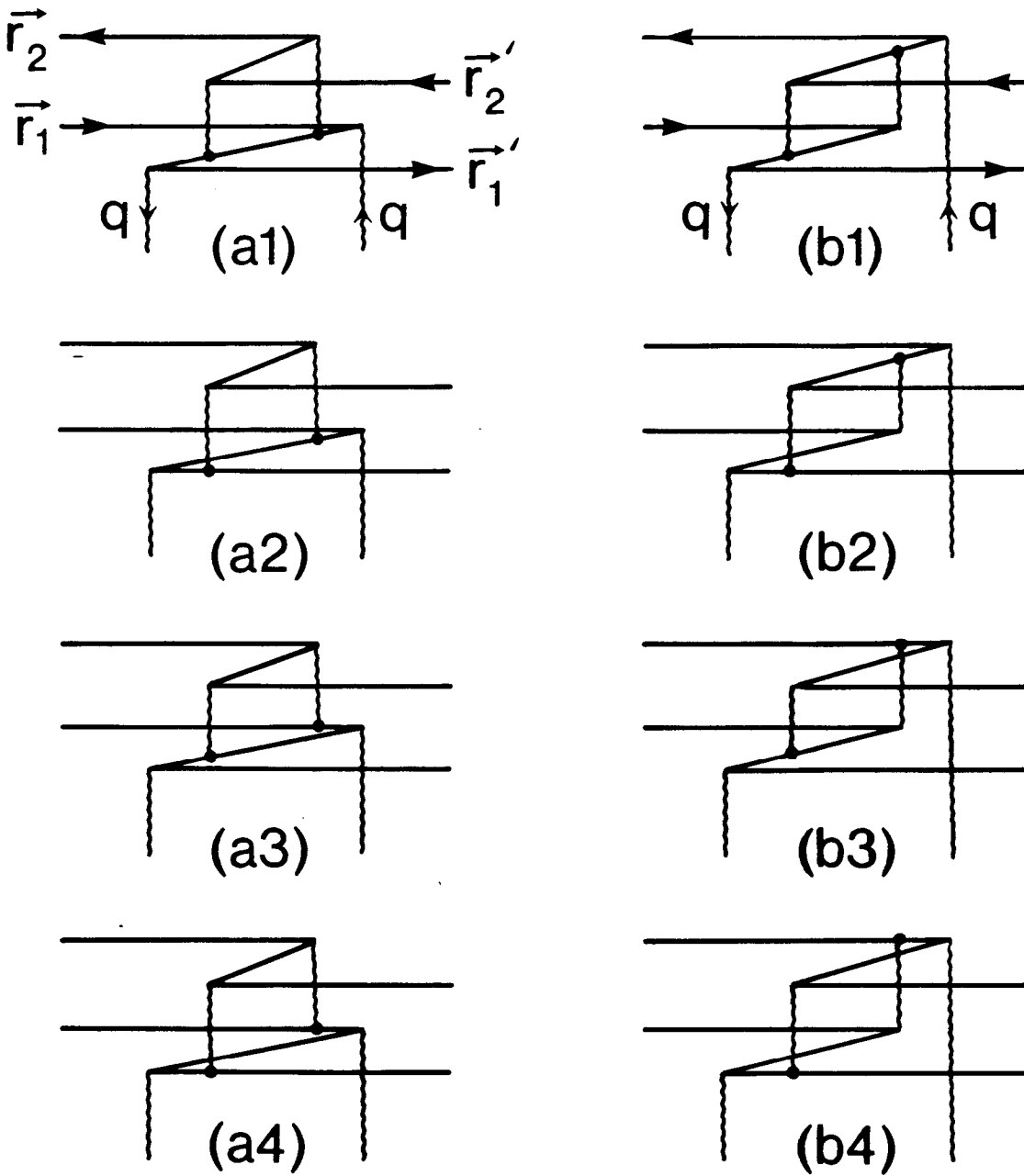


Fig. 4

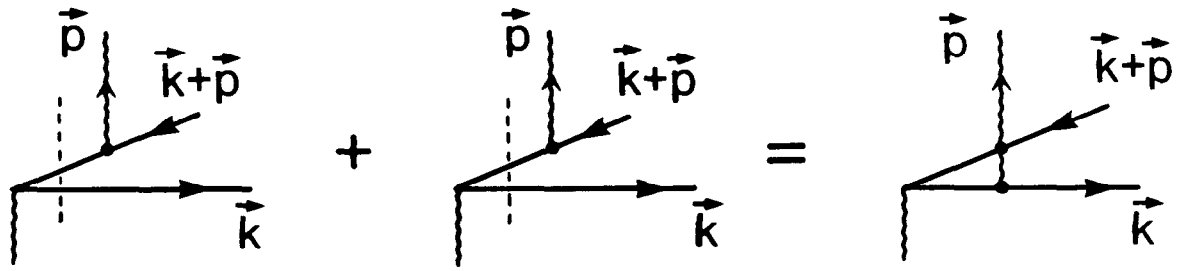


Fig. 5

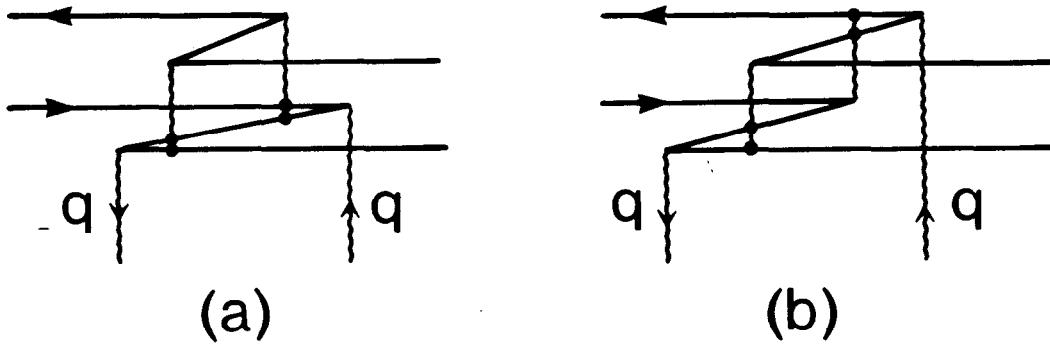


Fig. 6

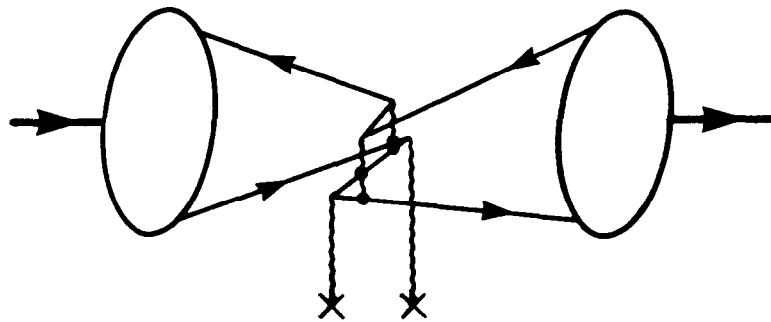
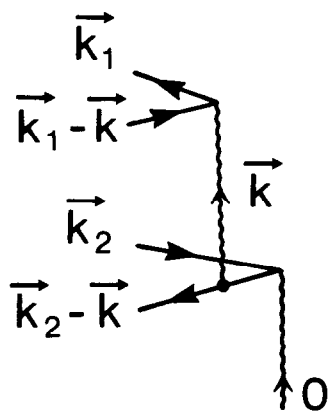
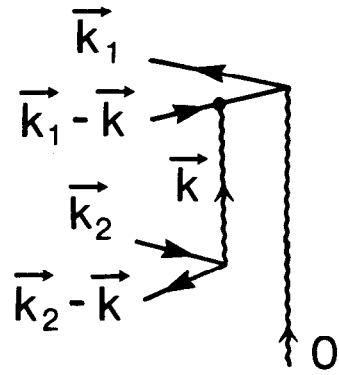


Fig. 7



(a)



(b)

Fig. 8

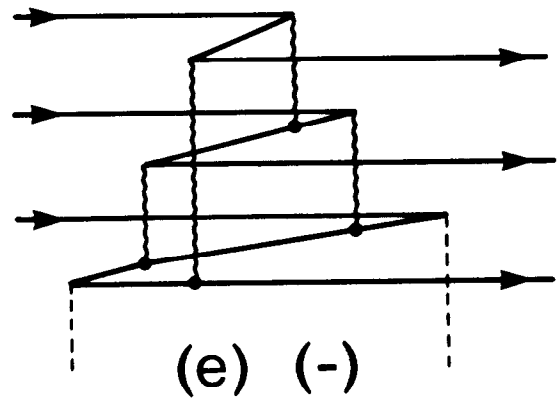
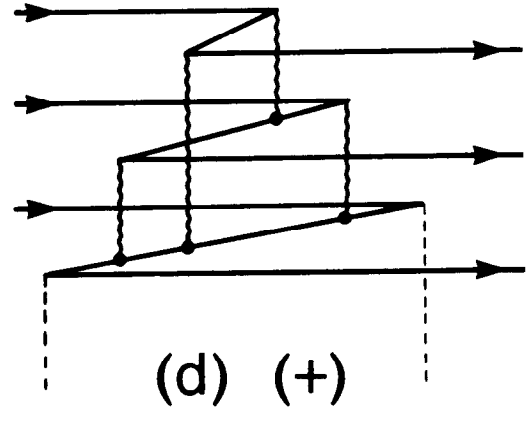
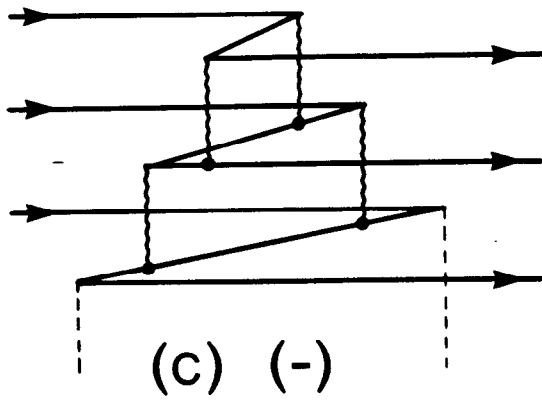
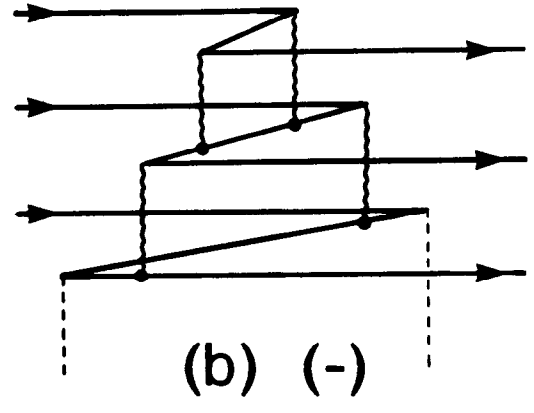
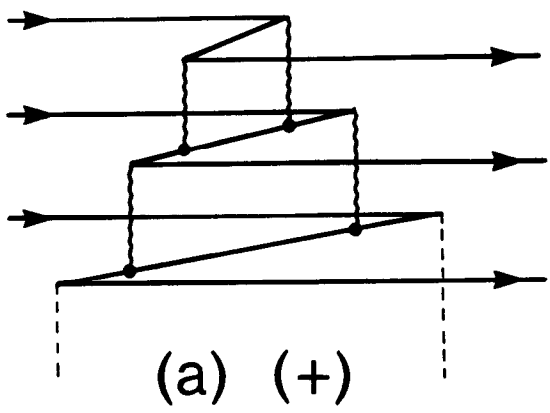


Fig. 9 .....

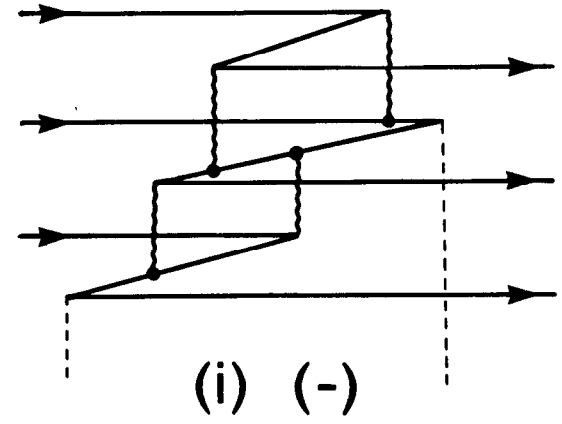
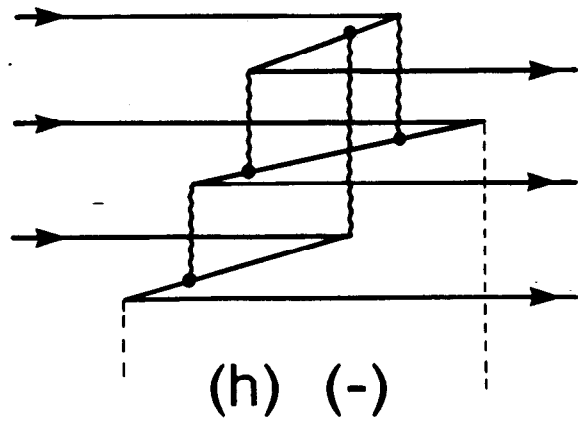
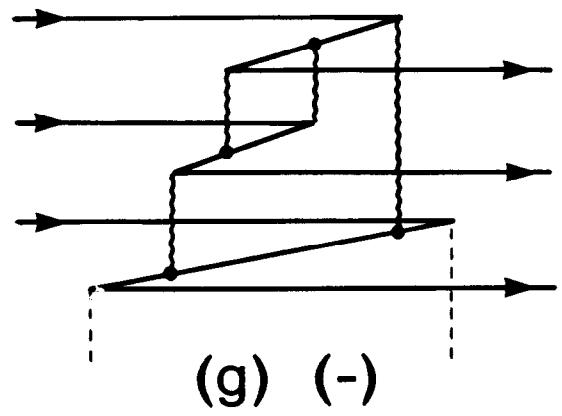
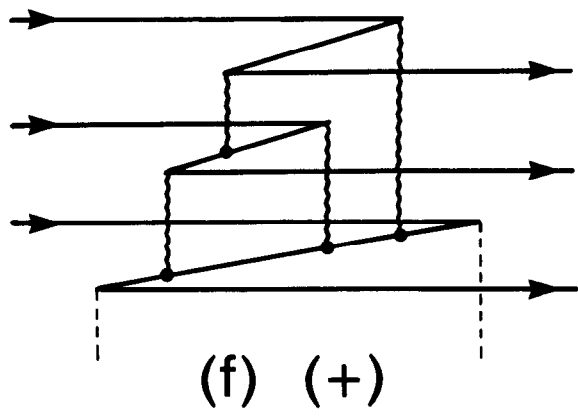


Fig. 9 (continued)

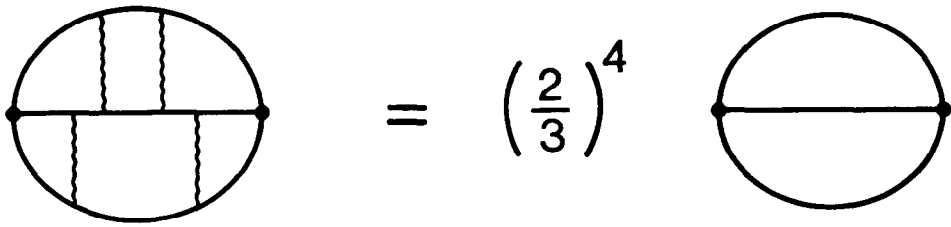


Fig. 10

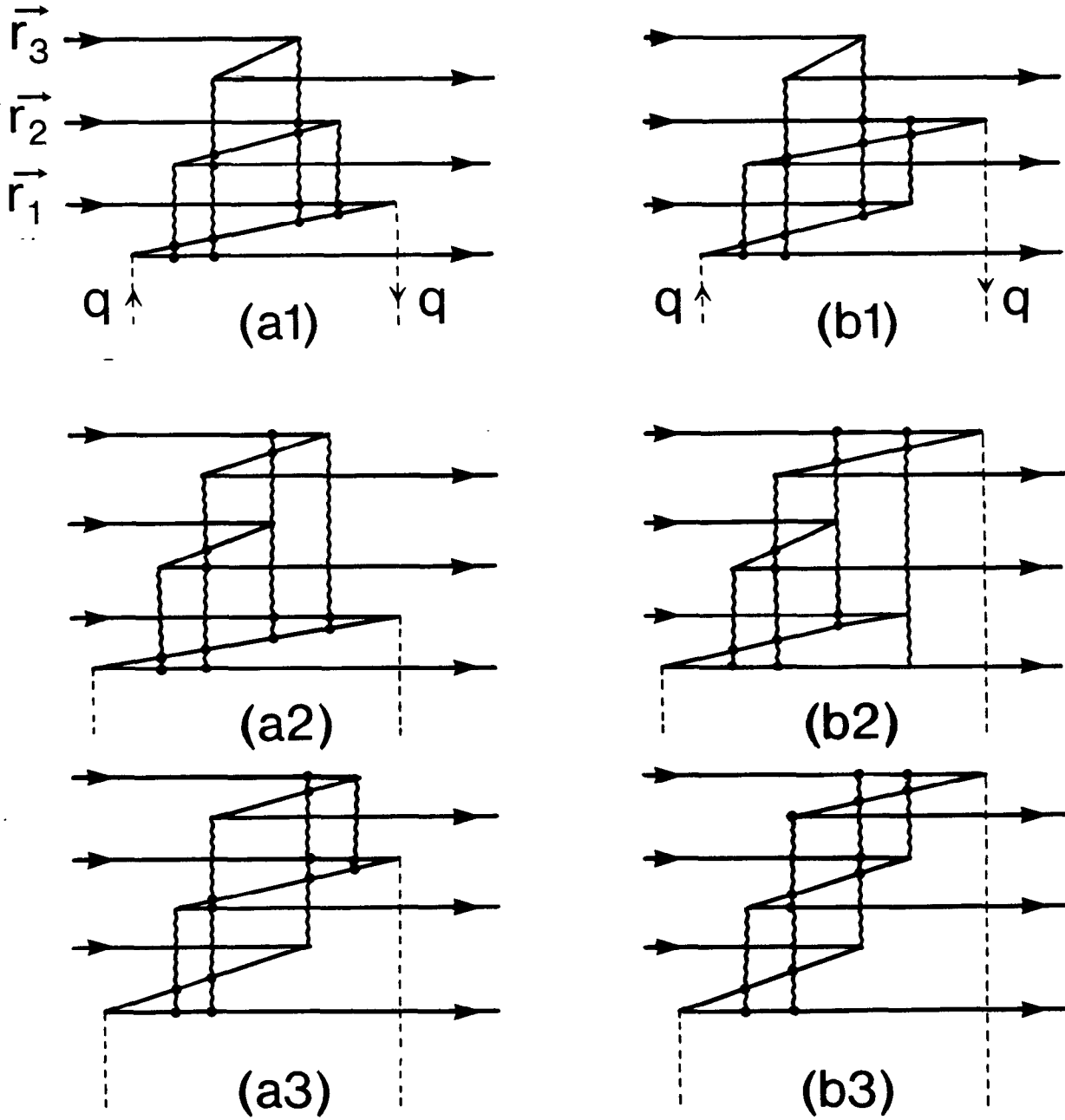


Fig. 11

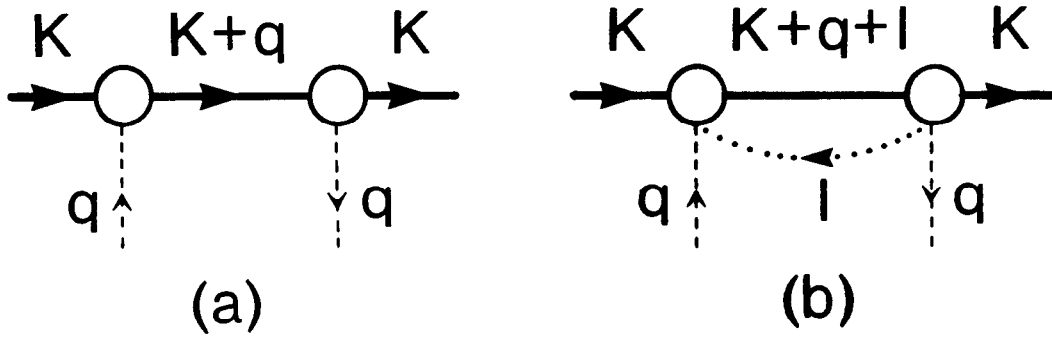


Fig. 12

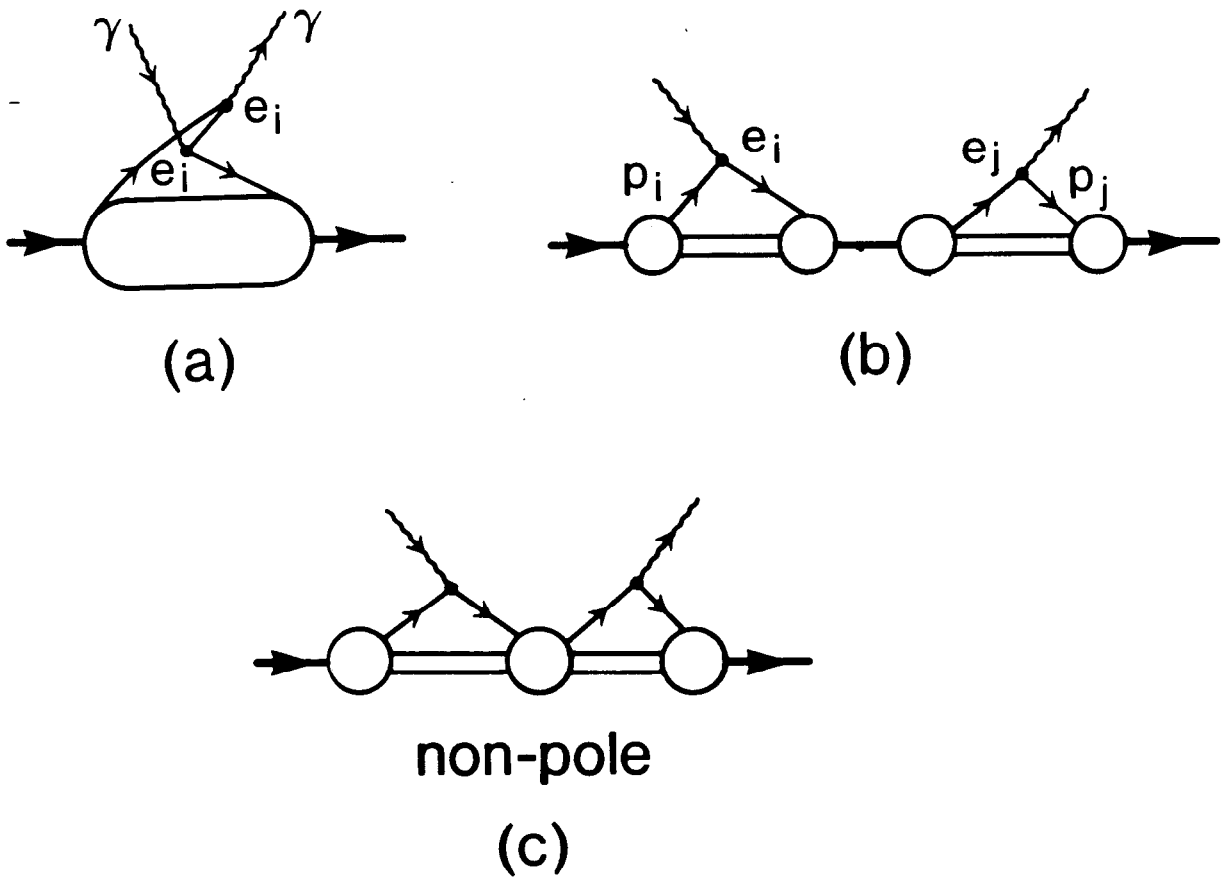


Fig. 13